

Thermal response of a magneto-structural material under an applied magnetic field

Author: Pau Garcia Pujol

Facultat de Física, Universitat de Barcelona, Diagonal 645, 08028 Barcelona, Spain.

Advisor: Antoni Planes

Abstract: We have studied a 2D model for a magneto-structural material that successfully simulates the behaviour of Fe-Pd multiferroic material. We have obtained configurations of magnetic and structural domains for selected values of the applied magnetic field. The model has provided us the necessary data to obtain the entropy change induced by application of a magnetic field. We have further tested the response of the system as we applied a saturation field that rotates in the xy plane

I. INTRODUCTION

Currently there is an increasing interest in technologies that explode solid state physics like ferroic and multiferroic materials. These materials exhibit interesting functionalities with enormous potential for technological applications such as refrigeration and shape-memory based devices among others. This kind of phenomena are usually linked up with a phase transition, and associated with a strong interplay between different ferroic properties such as strain, magnetization, polarization...

In our work we have simulated a magneto-structural alloy that undergoes a structural phase transition that drives a strong interplay between magnetization and strain in the low temperature phase.

We have used a magneto-structural model developed in reference [1]. Recently the model has proven to have high potential in the study of caloric effects involving strain and magnetization [2].

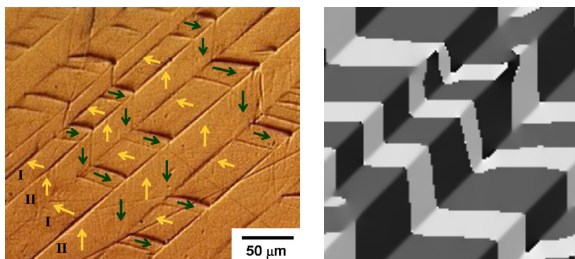


FIG. 1: comparison between (a) experimentally observed micro-magnetic structure in Co-Ni-Ga alloy. (b) Stable magnetic configuration obtained by numerical simulation.

Fig.1 illustrates the fitting between a real system and the numerical simulation of the model, picture (a) reveals the micro magnetic structure experimentally observed of a Heusler alloy, we can see the structural domains (Twins) denoted by I and II, and the magnetic stripes above, forced to point in the easy magnetization direction (direction that depends on the twin). Image (b) is a stable configuration obtained by a numeric simulation, in which the same micro-magnetic structure is observed.

The aim of this work is the study of magneto-caloric effects as we subject our system into a structural transition and the application of magnetic fields.

II. MAGNETO-STRUCTURAL MODEL

The model we simulated consists of a 2-D periodic boundary lattice in which each cell can be deformed and has an intrinsic magnetic moment with a rotation degree of freedom. We aim at studying a phase transition between a high temperature cubic phase with no restrictions for the spin orientation, and a low temperature rectangular phase with strong restrictions for the spin direction.

The total free energy of the model will have the following three contributions: a pure structural term (f_e), a pure magnetic term (f_m), and a term accounting for the magneto-structural interplay (f_{int}).

$$f = f_e + f_m + f_{int} \quad (1)$$

Additionally, we considered short range terms and long range terms. The second ones were treated in the Fourier space for the numerical simulations.

This model has many terms that compete when the free energy is minimized. Describing each one in detail would take very long. I will emphasize in the ones that better characterize the observed phenomenology.

A. Structural contribution

It is known that in a two dimensional cubic lattice there are three modes of deformation, the symmetry-adapted strains e_1 , e_2 and e_3 . In our case $e_2 = e = e_{xx} - e_{yy}$ describes the deformation in the low temperature phase. Thus we used it as the order parameter to describe a first order transition with the symmetry $e \leftrightarrow -e$. The structural free energy has the following contributions:

$$f_e = \frac{\alpha(T - T_c)}{2} e^2 + \frac{\beta}{4} e^4 + \frac{\gamma}{6} e^6 + \frac{\kappa}{2} |\nabla e|^2 + f_{e_1 e_3} + f_\eta \quad (2)$$

$\alpha, \gamma, \kappa > 0$ and $\beta < 0$ are the terms according to a Ginsburg free energy to obtain a transition at $T = T_c$. We also included a gradient term responsible for the formation of domains (or variants) accounting the minimization of ∇e (the strain variation along the lattice).

The quenched-in disorder (f_η) is introduced here as a tool that allowed us to relax the system into a given local deformation. Therefore we used it as a random perturbation to provide nucleation sites and help the system to undergo the phase transition.

$$f_{e_1 e_3} = \int \left(\frac{A_1}{2} e_1(r)^2 + \frac{A_3}{2} e_3(r)^2 \right) \quad (3)$$

If lattice integrity is imposed (absence of dislocations) e_1, e_2 and e_3 are not independent. They are constrained by the St.Venant relations. Minimization of the free energy under this condition enables to write this elastic energy as (in Fourier space):

$$f_{e_1 e_3} = \frac{A_3 A_1}{8\pi^2} \int \frac{(k_x^2 - k_y^2)^2 e(k) e(-k)}{8A_1 k_x^2 k_y^2 + A_3 (k_x^2 + k_y^2)^2} dk \quad (4)$$

eq.4 is interesting thus is minimized for $k_x = \pm k_y$. This condition explains the formation of twin domains along the diagonals of the square lattice.

B. Magnetic contributions

As indicated before, each cell has its magnetic moment, which can change its orientation but always remaining with the same modulus. For the magnetic contributions we proposed:

$$f_m = J|\nabla m|^2 - \frac{1}{2}\mu_0 M_s H_{ext} m - \frac{1}{2}\mu_0 M_s H_d m \quad (5)$$

The first term ($J|\nabla m|^2$) is an exchange energy term according to a ferromagnetic behaviour. The second and third term stands for the coupling with an externally applied magnetic field (Zeeman term (H_{ext})), and the demagnetization field (H_d), a term minimized when the magnetic lines are closed. This field carries the long range interactions between the magnetic moments.

C. Magneto-Structural contribution

At last we introduce the magneto-structural coupling.

$$f_{int} = \frac{B}{\sqrt{2}} (m_x^2 - m_y^2) e \quad (6)$$

As we can see in eq.6, there are two differentiated situations. In the high temperature phase $e = 0$ so the

energy contribution is zero independent on the magnetization. At low temperature the deformation can be both e or $-e$, in which case to minimize the free energy the magnetization would take the direction suitable to make this term the most negative (minimum). These are the easy magnetization directions, direction x for $-e$ strain and y for e strain.

III. DYNAMICS

The aim of this model was the visualization of the dynamics involved in a relaxation process. On one hand, the stable strain configurations are reached by means of pure relaxational dynamics, which consist in applying the following dynamical equation over all the unit cells.

$$\frac{\partial e_2(r)}{\partial t} = -\frac{\partial F}{\partial e(r)} \quad (7)$$

It is easy to see that the application of equation 7 will always bring the system to decrease its energy: $\frac{\partial F}{\partial t} = \frac{\partial F}{\partial e} \frac{\partial e}{\partial t}$ and using the relation above $\frac{\partial F}{\partial t} = -\left(\frac{\partial F}{\partial e}\right)^2 < 0$

In the other hand, the magnetic configuration evolves according to the Landau-Lifshitz-Gilbert (LLG)

$$(1 + \alpha^2) \frac{\partial m}{\partial t} = -\gamma_0 m \times H_{eff} - \gamma_0 \alpha m \times (m \times H_{eff}) \quad (8)$$

$$H_{eff} = -\frac{1}{\mu_0} \frac{\partial F}{\partial m} \quad (9)$$

Equation 8 has two contributions, the first term comes from the conservation of the angular momentum, and forces the spins to precess around the effective magnetic field, the second term is a phenomenological damping term experimentally observed, the spins reduce its precession until they align to the effective field.

Notice that the magneto-elastic coupling contributes to both dynamics, which will give correlations between magnetic and elastic configurations.

IV. THERMODYNAMICS OF MAGNETO-CALORIC EFFECTS

Caloric effects occur in any macroscopic system as a consequence of the variation of the generalized displacement variables (in our case the order parameters e and m) in relation to their conjugated fields. In the present work we have studied the caloric effects associated with the application of a magnetic field. When the field is applied isothermally the resulting entropy change is given by [3]:

$$\Delta S(T) = \mu_0 \int_0^H \frac{\partial M}{\partial T} \partial H \quad (10)$$

Were M is the magnetization in the direction of H . From our model we have computed this entropy change for applied fields up to the saturation field H_{sat} . This field is a field high enough to relax the system into a magneto-structural single-domain for the lower temperature limit ($T=0.55T_c$)

The caloric effects are especially interesting in the so called multiferroic materials where there is an interplay between the generalized displacements, as in our case were the magnetic field will not only affect the magnetization, but the strain too.

V. METHODOLOGY

We worked on a 128x128 two dimensional lattice of a $Fe_{70}Pd_{30}$ alloy, in which the spins may remain in the planar direction. The numerical parameters that describe this system are presented in table 1, but for the simulations the model has been described in reduced units.

symbol	value (S.I.)	symbol	value (S.I.)
T_c	257 K	M_s	$1.08 \cdot 10^6 \text{ A m}^{-1}$
α	$2.4 \cdot 10^8 \text{ N m}^{-2} \text{ K}^{-1}$	J	$10^{-13} \text{ N m}^{-2}$
β	$1.7 \cdot 10^{13} \text{ N m}^{-2}$	B	$-1.85 \cdot 10^8 \text{ N m}^{-2}$
γ	$3 \cdot 10^{16} \text{ N m}^{-2}$	A_1	$14 \cdot 10^{10} \text{ N m}^{-2}$
κ	$3.53 \cdot 10^{-9} \text{ N}$	A_3	$28 \cdot 10^{10} \text{ N m}^{-2}$

TABLE I: values in S.I. of the parameters of the model. Extracted from Ref [1]

In the present work, to obtain suitable results for the consequent thermodynamic analysis we only needed the equilibrium configurations as we applied a magnetic field in a quasi-static process. For this, the system is let evolve numerically until it reaches a stable configuration, according to a convergence criteria.

The first process analysed was the application of a magnetic field in the x direction, which is also the easy magnetization direction for the $-e$ strain. Our parameter of interest in this case will be m_x , as it is parallel to the applied field. We did this for a huge amount of temperatures and applied fields, since the thermodynamic equation reduced to a discrete space (eq.11) involves finite differences and integrals that needed to be accurately evaluated.

$$\Delta S(T) = \mu_0 \sum_0^H \frac{M(T + \Delta T) - M(T)}{\Delta T} \Delta H \quad (11)$$

After that, we proceed to study the behaviour of the system when the applied field rotates from x to y direction. We have done this for a saturation field, in order to force the system to switch its strain due the strong magneto-elastic coupling.

VI. RESULTS

A. Preliminary results, stable configurations

In this section I will present snapshots of magneto-structural stable configurations for selected temperatures and magnetic fields. The spin directions are represented in a grey scale in order to exhibit the spin directions in each region of the system, Fig. 2 image(a) represents the shade associated with each direction of the spin (in radial directions).

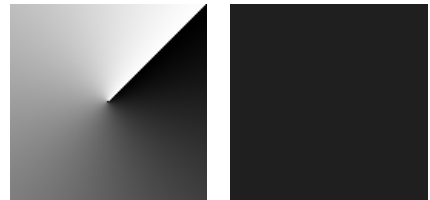


FIG. 2: (a) Spin radial direction according shade. (b) High temperature phase magnetic structure $T = 1.2$ $H = 0.01$.

As we see in Figure 2 (b), in the high temperature phase the values for strain and magnetization are $e = \langle e \rangle = 0$ and $m_x = 1$. The saturation appears for low values of the applied field as there is no restrictions for the magnetic moments being aligned along the field.

Figure 3 correspond to different stabilized states of the low temperature phase. For its according magnetic field. In the low temperature phase, due the strong coupling, magnetization and strain are highly correlated.

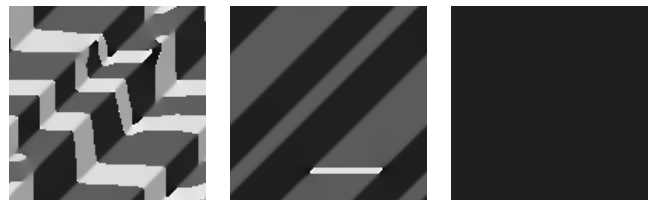


FIG. 3: low temperature phase magnetic configurations $T = 0.6$ (a) $H_a = 0.01$, (b) $H_b = 0.10$, (c) $H_c = 0.30$

Figure 3 (a) shows a twinned structure in which the magnetization has formed stripes. This occurs for low values of the magnetic field whereas the demagnetizing field has the most relevant magnetic contribution. For this case we will have $e \neq 0$ and $\langle e \rangle \simeq 0$, $\langle m_x \rangle \simeq 0$.

If Figure 3 (b) the magnetic field was raised to the point that the energy associated with the external field was more significant than the demagnetization field. For this case, the magnetic stripes were eliminated, but the twinned elastic configuration still reminded. As result, each twin resulted in a magnetic mono-domain. For this configuration we had $e = \langle e \rangle \neq 0$, $\langle m_x \rangle \simeq \frac{m_{sat}}{2}$.

In Figure 3 (c) the system was saturated in both strain and magnetization $e = \langle e \rangle \neq 0$, $\langle m_x \rangle = 1$ which resulted

in a magneto-structural single-domain that looked like the high temperature phase. This is the so called magnetic saturation that is reached when $H = H_{sat}$.

B. Thermodynamic study

For the first analysis we provided a large number of points for magnetization in front both temperature and applied field, figure 4 shows this data set as a three dimensional surface.

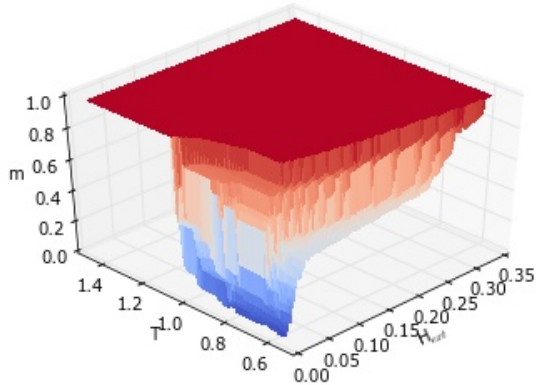


FIG. 4: Magnetization vs T and H

For an easier visualization of that data we displayed the results as 1D profiles. Figure 5 shows the magnetization profile versus temperature for selected values of applied field. The saturation field is determined as the field that will give us magnetic saturation $\langle m_x \rangle = 1$ for all temperatures. This value stands around $H \simeq 0.33$. Thus, this was our upper limit in the entropy calculation.

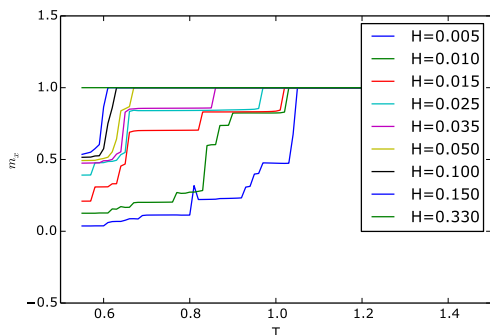


FIG. 5: magnetization vs.temperature

In Figure 5 we can observe the behaviour of the magnetization depending on H values. As the external field decreased the magnetization vary from $\langle m_x \rangle = 1$ to approximate $\langle m_x \rangle = 1/2$. This occurs because the magnitude of the structural free energy (which have a strong

dependence in temperature) is more important than the magnetic energy. At this point, we recovered the twinned structure, and the spins were forced to change its directions. For the lowest values of the external field the magnetization drooped to $\langle m_x \rangle = 0$. At this point stripes were observed as well.

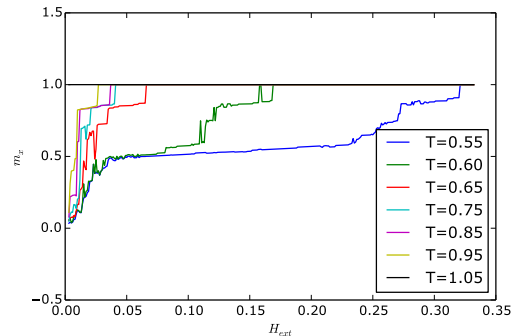


FIG. 6: magnetization vs. H

Figure 6 represents the magnetization dependence on H for different temperatures values, this profiles were the ones that take our interest, since this were the ones used to determine the entropy change. From eq.11, the area contained between two consecutive profiles gives us the differential entropy change in the range between T and $T + \Delta T$

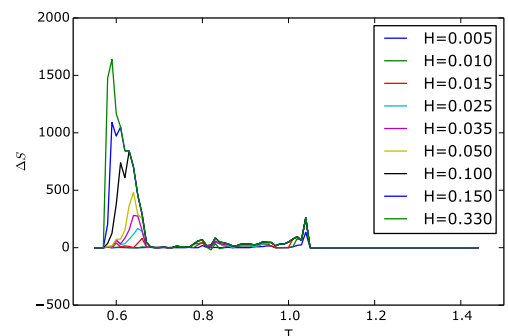


FIG. 7: entropy gain

Fig.7 gives the entropy obtained from the simulation results. We can see that each profile has two peaks that get closer as the field is increased and finally they superpose. This behaviour could be determined by the magnetic transformation between the stable configurations shown before (Figure 3). While the first peak always appears at low temperature, the second one has a higher dependence on the applied field.

We have calculated an average entropy change (Figure 8) for each externally applied field. It is obtained as:

$$\langle \Delta S \rangle = \int_0^T \frac{\Delta S}{\Delta T} \partial T, \quad (12)$$

where ΔT is the temperature interval of the entropy change peaks in figure 7. This average entropy change is an increasing function that reaches an upper limit for the saturating value of the field $H = H_{sat}$. This increase is a striking behaviour that can be explained taking into account the magneto-structural interplay. It is related to an inverse magneto-caloric effect [4] that is consistent with the decrease of magnetization at the transition from the high to the low temperature phase (see Fig.5).

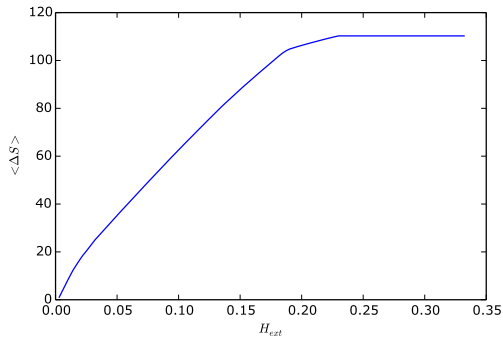


FIG. 8: main entropy gain

C. rotatory field

The results presented in this section here consist of a description of the behaviour of the system as the magnetic field completes a 360 rotation. In the next figures we present the magnetization and strain evolution according to the angular direction of the magnetic field.

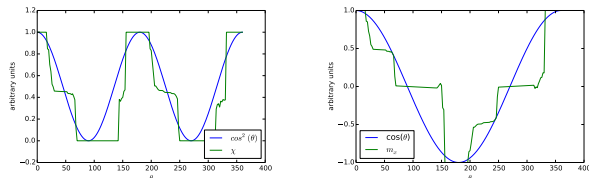


FIG. 9: (a) fraction of transformed strain,
(b) magnetization

Figure 9 (a) corresponds to the transformed fraction of strain, the rate of cells that have $-e$ strain. Its a fact that this function goes from 0 to 1, thus we have presented them within the quadratic cosine of the angle.

Figure 9 (b) corresponds to $\langle m_x \rangle$, since its values can go from 1 to -1 and should be aligned with the field we have represented them within the cosine. This preliminary results open new routes in order to study magneto-caloric effects under rotating fields in the future.

VII. CONCLUSIONS

The model presented in this work showed its capability to reproduce the physics involved in multiferroic materials that display strong magneto-structural interplay, and proven worth as a tool to obtain stable configurations induced by changes in temperature, stress and magnetic field. The magneto-caloric study has shown the expected results. Figure 7 indicates that the most significant contribution to it appears at the lowest temperatures. Although the main entropy change has revealed a jerky evolution, its origin remains not completely understood. We suggest that it can be related to system size effects or to the strong magneto-structural interplay among others possibilities that will be analysed in detail in the future. This jerky evolution is also clearly seen in the rotatory field results. For further studies I would propose the optimization of the numerical algorithm in order to decrease its computation time.

VIII. ACKNOWLEDGEMENTS

I want to thank my tutor Antoni Planes and my mate Jonathan Gebia for their support and so valuable help.

- [1] POL LLOVERAS *interplay between anisotropy and disorder in ferroelastics: structures and thermodynamics*, PhD Thesis, Barcelona, 2010.
 [2] TISHIN A M *Magnetocaloric effect in the vicinity of magnetic phase transitions*, *Handbook of Magnetic Materials vol12*, Amsterdam, 1999.

- [3] M. ACET, L. MAOSA AND A. PLANES *Handbook of magnetic materials vol 19*, Amsterdam, 2011.
 [4] M. ACET, L. MAOSA AND A. PLANES *Magnetocaloric effect and its relation to shape-memory properties in ferromagnetic Heusler alloys.*, Amsterdam, 2011.